ICES Journal of Marine Science

ICES Journal of Marine Science (2015), 72(8), 2494–2505. doi:10.1093/icesjms/fsv077

Original Article

Measuring *in situ* krill tilt orientation by stereo photogrammetry: examples for *Euphausia superba* and *Meganyctiphanes norvegica*

Rokas Kubilius[1,2,3]*, Egil Ona[2], and Lucio Calise[2]

[1]*Metas AS, Nedre Åstveit 12, 5106 Øvre Ervik, Bergen, Norway*
[2]*Institute of Marine Research, PO Box 1870 Nordnes, NO-5817 Bergen, Norway*
[3]*Department of Biology, University of Bergen, PO Box 7803, N-5020 Bergen, Norway*

**Corresponding author: tel: +47 90 36 09 03; fax: +47 55 23 85 31; e-mail: rokask@metas.no*

Kubilius, R., Ona, E., and Calise, L. Measuring *in situ* krill tilt orientation by stereo photogrammetry: examples for *Euphausia superba* and *Meganyctiphanes norvegica*. – ICES Journal of Marine Science, 72: 2494–2505.

Received 12 January 2015; revised 27 March 2015; accepted 10 April 2015; advance access publication 12 May 2015.

The natural body orientation adopted by krill is a crucial parameter for understanding and estimating the acoustic backscattering from these animals. Published data are scarce and are usually acquired with single camera systems that provide suboptimal control over the measurement accuracy. Here, we describe a stereo photo camera application for accurate krill measurements *in situ*, based on several *Euphausia superba* and *Meganyctiphanes norvegica* datasets. Body tilt orientation, body length, and school volume density from scattered and schooling krill are presented. Some challenges to the practical implementation of the method are discussed, including practical limits on krill body yaw angles for obtaining useful measurement accuracy and how to account accurately for the true vertical. Calibration and measurement accuracy is discussed together with a practical definition of krill body orientation. Krill sizes determined from stereo images are compared with those measured from trawl samples. The krill body tilt measurements yielded mean estimates of positive (head-up) or negative tilt of 9–17° with rather large spread for scattered aggregations of *M. norvegica* ($SD = 30–37°$) and about half of that for polarized schools of *E. superba* ($SD = 14–17°$). The measured krill body orientation distributions were also used to calculate krill acoustic target strength as predicted by the stochastic distorted wave Born approximation (SDWBA) model.

Keywords: *Euphausia superba*, krill, *Meganyctiphanes norvegica*, orientation, stereo camera, stereo photogrammetry, tilt, underwater photography, zooplankton, zooplankton acoustics.

Introduction

Euphausiids (broadly referred to as krill) are key species in many ocean ecosystems (Mauchline and Fischer, 1969; Mauchline, 1980). A good example is the Antarctic krill (*Euphausia superba*, Dana, 1852), which is the most important component of the Southern Ocean foodweb (e.g. Hopkins *et al.*, 1993; Lancraft *et al.*, 2004) with annual predator consumption of 128–470 million tonnes per year (Atkinson *et al.*, 2009). Northern krill (*Meganyctiphanes norvegica*, Sars, 1857) is the most abundant of the krill species in the North Atlantic and associated seas (Einarsson, 1945; Mauchline and Fischer, 1967; Tarling *et al.*, 2010). It is also an important food source for many fish species, whales, and seabirds with a total predation rate up to 200–400 million tonnes per year (Simard and Harvey, 2010; Tarling *et al.*, 2010). Both Antarctic and Northern krill are important components of many marine ecosystems and the need for regular monitoring of krill stock status is clear.

Acoustic methods provide a rapid and cost-effective way of sampling large water bodies when monitoring pelagic biological resources (Simmonds and MacLennan, 2005). Multifrequency techniques are now commonly used to separate the krill backscatter from that of other detected targets (e.g. Holliday *et al.*, 1989; Miyashita *et al.*, 1997; Watkins and Brierley, 2002; Woodd-Walker *et al.*, 2003). When converting the backscattered acoustic energy to biomass, the mean target strength (TS in dB re 1 m^2) of the ensonified krill must be known (Foote and Stanton, 2000). For fish, Nakken and Olsen (1977) and Haslett (1977) showed that TS varies greatly with the body posture, and thus measurements of natural body orientation distributions are needed to determine

the appropriate *TS* (Foote, 1980). Similar dependencies were indicated for euphausiids at higher acoustic frequencies (Greenlaw, 1977). More recently, the body orientation was suggested as one of the main causes of the variability in predicted and observed krill *TS* (e.g. Klevjer and Kaartvedt, 2006; Calise and Skaret, 2011; Calise and Knutsen, 2012), and the disparities (sometime >25 dB or two orders of magnitude) between empirical data and theoretical model predictions (e.g. Greenlaw *et al.*, 1980; Cochrane *et al.*, 1991; Stanton *et al.*, 1993; McGehee *et al.*, 1998; Demer and Conti, 2003, 2005). Behavioural patterns, such as the diel vertical migration of Antarctic (e.g. Zhou and Dorland, 2004; Cresswell *et al.*, 2009) and Northern krill (e.g. Onsrud and Kaartvedt, 1998; Kaartvedt, 2010), are likely to cause substantial changes in the mean body orientation adopted by the animal and consequently have a large effect on *TS*. Furthermore, fine scale studies (e.g. Sourisseau *et al.*, 2008; Vestheim *et al.*, 2014 for Northern krill) have revealed a quite complex structure of krill diel vertical migration, which is not limited to the bulk vertical displacement at dusk and dawn.

Euphausiid swimming orientation and body tilt have been directly examined in aquaria (Kils, 1981; Endo, 1993; Miyashita *et al.*, 1996; Letessier *et al.*, 2013) and *in situ* (Lawson *et al.*, 2006), with most reports concerning the Antarctic and Pacific krill (*E. superba* and *E. pacifica*), and mixtures of North Atlantic euphausiid species (Sameoto, 1980; Kristensen and Dalen, 1986). Measured body tilt angles are onwards conveniently described by fitted normal distributions, giving the mean and standard deviation in the notation $N(\bar{\theta}; SD_\theta)$ (Stanton *et al.*, 1993). Kils (1981) and Endo (1993) observed Antarctic krill in small aquaria and reported $N(45.3; 30.4)$ and $N(45.6; 19.6)$, respectively, which differ considerably from the *in situ* measurements ($N(9.7; 59.3)$) reported by Lawson *et al.* (2006). On the other hand, the results of Letessier *et al.* (2013) who used a much larger aquarium corresponded better to the *in situ* data (wrapped normal distribution mean 23.5°, $SD \approx 37°$). Kils (1981) is the only published *ex situ* dataset on Northern krill body tilts ($N(53.8; 64.2)$); again, this result differs from the *in situ* distributions reported by Sameoto (1980) and Kristensen and Dalen (1986) for Northern krill as part of multispecies krill mixtures. Krill body tilt distribution has also been estimated from acoustic backscatter modelling exercises with an inversion method by tuning the *TS* models to fit the volume backscattering data and krill body orientation being the output (e.g. Demer and Conti, 2005; CCAMLR, 2010; McQuinn *et al.*, 2013). Most of the model exercises concluded with narrower krill body tilt distributions compared with the empiric measurements, for example: $N(15; 5)$, $N(4; 2)$, and $N(11; 4)$ for *E. superba* (Demer and Conti, 2005; Conti and Demer, 2006), $N(9; 4)$ for *Thysanoessa raschii*, and $N(12; 6)$ for *M. norvegica* (McQuinn *et al.*, 2013). Only CCAMLR (2010) claimed a wider distribution $N(-20; 28)$ with negative mean, estimated revising the CCAMLR (Commission for the Conservation of Antarctic Marine Living Resources) Antarctic krill acoustic survey data from the year 2000 with an improved model (Calise and Skaret, 2011). In general, accurately and preferably *in situ* measured krill body orientation data are still scarce and such studies are very valuable.

The most common equipments used to quantify krill body tilt are single photo and video-camera systems. These can be sufficient to quantify krill body tilt in well-controlled environments such as aquaria, but potentially suboptimal for measurements of organisms *in situ*. The fraction of the encountered animals that can be measured by a single camera system is severely limited, since only animals observed more or less broad-side can be measured. It is also hard to evaluate which animals are observed broad-side, and is predominantly done "by eye". The main difficulty when using single camera systems for *in situ* krill body orientation measures is to properly account for camera system pitch and roll, which has a potential to introduce severe measurement bias. Lawson *et al.* (2006) used a pitch sensor of the towed body (equipped with a camera) to address this challenge, whereas Sameoto (1980) and Kristensen and Dalen (1986) present little to no evaluation of these errors.

Most of the single camera system shortcomings can be overcome or addressed better by using calibrated stereo cameras. These have been successfully applied in studies of marine animals, mainly fish (e.g. Cullen *et al.*, 1965; Klimley and Brown, 1983; Dolphin, 1987; Cappo *et al.*, 2007; Shortis *et al.*, 2009). In fact, the method has already been used to investigate krill schooling behaviour (Dolphin, 1987; Kawaguchi *et al.*, 2010). However, the methodology remains largely unused when it comes to the animal body orientation studies, with one exception. Letessier *et al.* (2013) used an underwater stereo video camera to measure krill orientation and size in a tank, as a brief demonstration of the method for proposed *in situ* application. In this study, we present a first example datasets of Antarctic krill (*in situ*) and Northern krill (*in situ* and *ex situ*) body-orientation measurements obtained by stereo cameras and analysed using stereo photogrammetry methods. We also discuss and address some of the practical method implementation challenges for the future use.

Material and methods

Free-swimming Antarctic and Northern krill were observed in four separate experiments (Table 1). Stereo photographs of Antarctic krill were collected in March 2008 not far from the Bouvet Island, South Atlantic Ocean by lowering the camera assembly from a drifting research vessel (from now on experiment A, "exp. A"). The example picture of schooling Antarctic krill is shown in Figure 1. While stereo photographs on dispersed and scattered Northern krill were collected in November 2010 and 2011 at locations in fjords close to Bergen, Norway: first, in a sheltered enclosure near the shore (2010, from now on "exp. B"), later by lowering the camera assembly from a stationary research vessel in 2010 and 2011 (from now on "exp. C" and "exp. D", respectively). The photo datasets were collected in conjunction with krill backscattering measurements made with narrowband and broadband sonars.

Stereo camera set-up, calibration, and measurement accuracy

The stereo camera system consisted of two identical 12.1 Mpx Imenco SDS 1210 underwater photo cameras, firmly mounted on a specially designed stainless steel frame providing stable mounting geometry. Two Imenco Flash 110 units were attached 0.5 m above the photo cameras for exp. B, C, and D, while only one flash was used in exp. A. The use of two flashes was necessary due to variable delay between the camera triggering times of up to 0.1 s (measured; average 0.037 s, $N = 79$). Krill has a relatively low average pleopod swimming speed of about one body length per second (Kils, 1981). This would translate to ~0.9 mm animal displacement in space between the capture time instances of the two pictures in a stereo pair, if calculated for the average size of the observed Northern krill. No escape reactions (rapid tail stroke with strong acceleration backwards, Kils (1981)) were observed during measurements or evident in all our data. For exp. B, C, and D data analysis, it was assumed that animal displacement in space was

Table 1. Overview of the four experiments providing stereo photos of Antarctic (exp. A) and Northern krill (exp. B, C, and D), and related trawl sampling.

Experiment	A	B	C	D
Location	S. Atlantic Ocean (54°34′27″S 004°58′11″E)	Austevoll Research St (60°05′17″N 005°15′55″E)	Osterfjorden (60°34′35″N 005°25′40″E)	Romarheimsfjorden (60°41′40″N 005°40′44″E)
Date	12–13 March 2008	05–07 November 2010	25–28 November 2010	01 December 2011
Local time	20:00–01:00	10:00–02:00	20:00–06:00	02:00–08:00
Camera depth (m)	20	4	10–30	65
Bottom depth (m)	2900	15	260	92
Measurements	*In situ*	*Ex situ* (mesocosm)	*In situ*	*In situ*
Trawl samples	1	4[a]	3[b]	1
Date	11 March 2008	25–26 October 2010	26–28 November 2010	01 December 2011
Local time	15:00	21:00–24:00	00:30–03:00	15:00
Depth (m)	25	20	10-17	60
Speed (m s^{-1})	1.1	1.3	1.4	1.4

[a]Live and healthy krill were sampled in Raunefjorden (60°16′N 005°09′E) using a Methot Isaac-Kidd ring trawl (mesh size 500 μm, modified codend) and transported to the experiment site within 1 h after the last catch.
[b]One trawl haul per image data collection night.

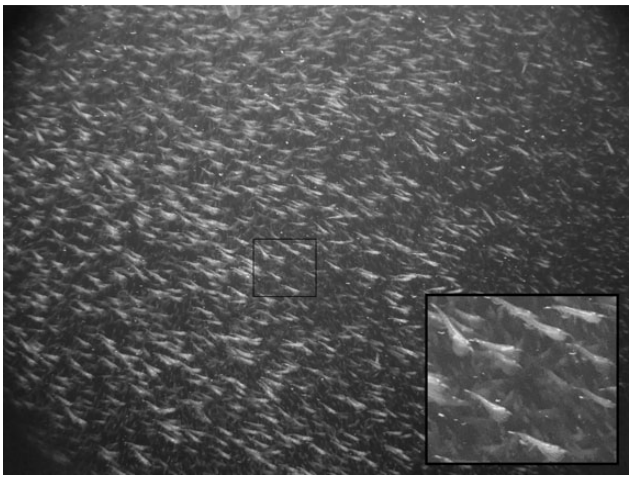

Figure 1. Example photograph of an Antarctic krill school observed by a stereo camera at 20 m of water depth (one image of the stereo pair).

negligible for the photos of one stereo pair. Both cameras were triggered manually by a single switch, with electrical communication and image transmission via underwater cables. The camera triggering frequency varied depending on krill occurrence, but generally a picture-pair was taken every 0.5–3 min. The stereo camera calibration and data post-processing were done with purpose-built SeaGis products: a calibration cube, a bar of known length (with length marks at 391.6, 853.4, and 1244.9 mm), the calibration software CAL (ver. 2.00), and measurement software PhotoMeasure (ver. 1.86) (SeaGis, 2014). The exp. A stereo camera calibration was performed after the data collection with acceptable quality, but had somewhat poorer measurement accuracy than in later experiments. The exp. B and C stereo camera calibrations were performed at the measurement sites at 3–4 m water depth. The camera calibration for exp. D was done just after data collection in a tank filled with seawater.

The body orientation and length measurements of krill were obtained by identifying two points on the same animal seen in both stereo pair images (image size 4000 × 3000 pixels), namely the anterior edge of the eye and the tip of the telson, and by extracting their absolute three-dimensional position. The animal length was determined as the distance between the two points in a three-dimensional space, while the body orientation was defined as the angle between the horizontal plane and the line passing the two reference points. The distance between the reference points, hereafter referred as AT length, is similar to the "AT" length defined in Morris *et al.* (1988) (Figure 2). This measure was chosen as the most practical for body tilt measurements on krill. When the image sharpness was not ideal, only the tilt angle was measured if the position of either of the reference points could not be determined exactly, thus substantially affecting the length measurement, but much less so the body tilt. While approximate eye contour was seen, the exact position of the anterior edge of the dark krill eye was not always easy to pinpoint against the black background of the sea. The krill was measured only when within 1.0–3.0 m of range from the cameras, and accepted for analysis only when the body yaw angle to the photographic plane was within $\pm 40^{\circ}$ (Figure 3). The characteristic euphausiid body shape was easy to identify. However, the species composition within the observed water layer had to be confirmed by trawl sampling near the data collection sites (Table 1). The same Antarctic krill body reference points were used when measuring trawl-catch krill body length in exp. A as in stereo image processing. A differently defined body length was used when sizing trawl catches in exp. B, C, and D, following the standard procedures on research vessels of the Institute of Marine Research (Norway); this is the length from the rostrum tip to the posterior end of the terminal spine at the end of telson, or length "TT" as in Morris *et al.* (1988). The conversion formula $AT = 1.036 \times TT + 0.374$ [revised after Calise (2009)] was used to enable a rough comparison of the Northern krill body length estimates. The mean animal body tilt, length, and corresponding standard deviations were obtained from the least-squares fitted normal distributions.

The target range from the camera and krill body yaw angle limits were based on the work of Harvey *et al.* (2002) and our empirical measurements. Harvey *et al.* (2002) showed that for optimum accuracy and precision of stereoscopic fish *length* measurement the target should be $<60^{\circ}$ off the photographic plane and at no more than 75–85% of the maximum visibility range (measured on 120–880 mm length fish models). More challenging was to evaluate the accuracy of *tilt* measurements and the yaw cut-off angle for

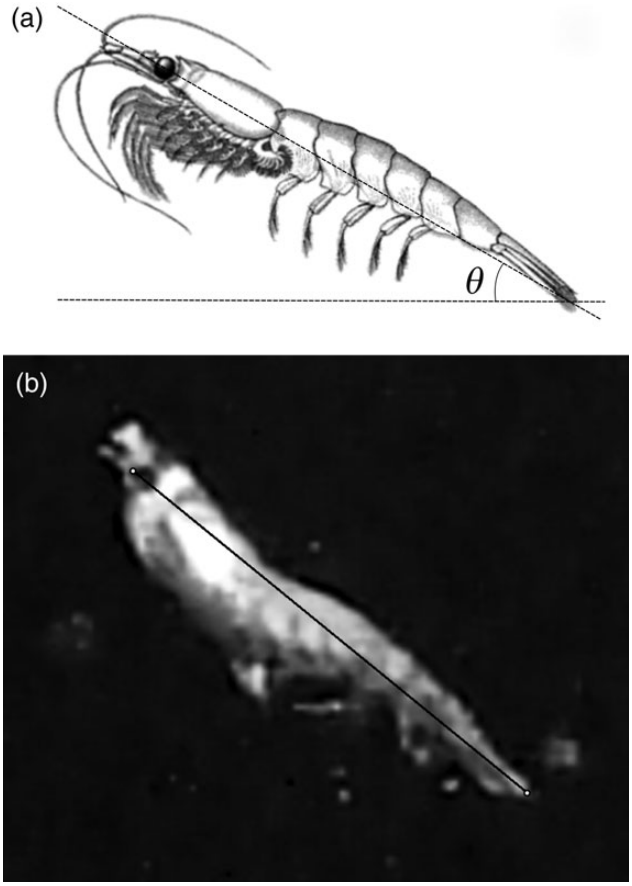

Figure 2. (a) Drawing of Northern krill [modified after G. M. Woodward *in* Holt and Tattersall (1905)] with tilt angle θ definition. (b) Example picture of free-swimming Northern krill with close to maximum yaw angle for acceptable measurements ($\leq 40^\circ$; zoomed in; exp. A). Black line is length from anterior edge of eye to tip of telson (referred to as length AT in the text). The tilt, yaw angle, and length of this animal were 33.0°, 35.3°, and 26.2 mm, respectively.

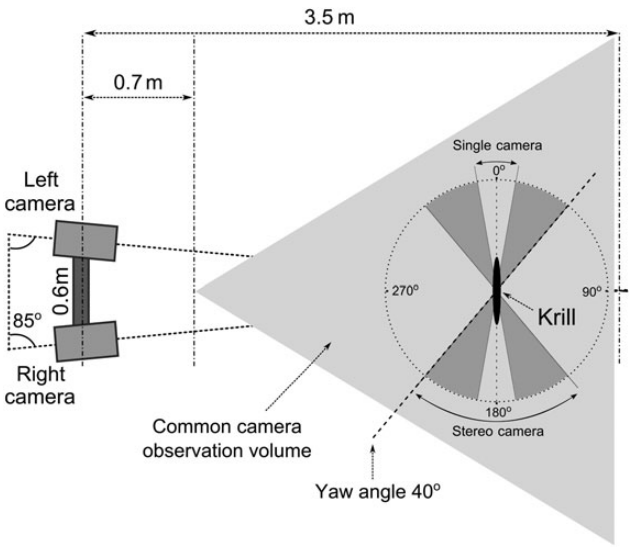

Figure 3. Stereo camera geometry viewed from above (not to scale). The range of acceptable krill body yaw angles ($\pm 40^\circ$) is also illustrated and visually compared with one acceptable for single camera-based measurements.

reliable tilt/length measurements. This was investigated by an experiment performed *in air* with good light conditions. The test object was a matchstick mounted on a protractor and inclined at 15° (with 1° accuracy) simulating the tilt of that magnitude and two length marks 30.0 mm apart (0.1 mm accuracy; Figure 4a). It was placed on a flat, marked with lines, surface at multiple positions and distances (0.9–1.4–2.3 m) from the stationary, laterally observing stereo camera (calibrated in air). Tilt and length measurements were made with the test object placed first in the photographic plane (0° yaw angle; Figures 3 and 4a), then with increasing, less favourable yaw angles up to $\pm 70^\circ$ with 5° steps. The extreme yaw angles would simulate krill swimming roughly towards or away from the camera. The mean measured test object tilt from horizontal and length were 15.4° ($SD = 0.9^\circ$, $N = 90$) and 30.0 mm ($SD = 0.4$, $N = 90$), respectively, close enough to the known tilt and length (Figure 4b and c). The measurements were little affected by yaw angles of the test object within the range $\pm 50^\circ$, while somewhat higher variability was observed at more extreme yaw angles. It appeared that the body tilt measurement is accurate provided the animal contour is clearly seen which, with our equipment, we associated with yaw angles within $\pm 40^\circ$. The length measurement accuracy was also confirmed empirically by measuring length of a known calibration object in water during or after the actual data collection. This determined the length accuracy to be about ± 1.6, ± 0.5, ± 1.5, and ± 1.1 mm in exp. A, B, C, and D, respectively. The deviation of the length measurement accuracy from the in-air experiment was likely caused by slight changes in the geometry of the camera internal parts while handling and redeploying the stereo camera unit.

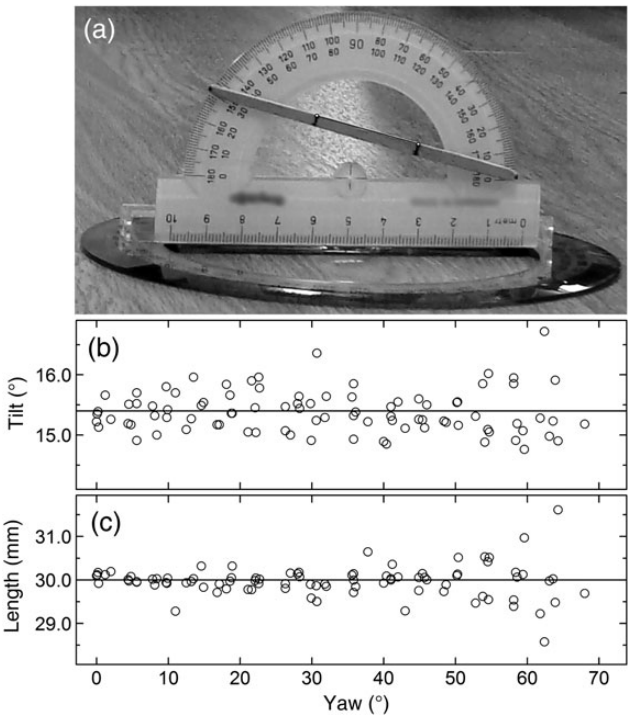

Figure 4. (a) The test object: a large matchstick glued at an angle of 15° onto the side of a 180° protractor, which in turn is attached perpendicular to a 360° protractor. The measured test object tilt (b) and length (c) are shown for object yaw angles from zero degrees (like in a) up to 70°. Black lines in b and c indicate the mean value.

In situ exp. A, C, and D

Three *in situ* photographic datasets were obtained: one during a survey on Antarctic krill by RV "G.O. Sars" (2008, exp. A) and two datasets on Northern krill during in-fjord experimental acoustic surveys by RV "G.O. Sars" (2010, exp. C) and RV "Håkon Mosby" (2011, exp. D; Table 1). The stereo camera assembly was mounted for horizontal viewing on an acoustic probe (1.7 m high, Ø1.3 m, and weight 700 kg). The probe was deployed on armoured optical cable, which was also used for real-time communication and signals triggering the cameras (Figure 5a). In the exp. A, the probe was operated at 20 m depth with a stereo camera attached to a motorized plate at the lower part of the probe. The plate was equipped with a pitch and roll sensor (EZ-Compass-3) and could be manipulated to set the stereo camera system pitch and roll to zero degrees (i.e. horizontal) while at the measurement depth. For exp. B, C, and D, plumb-line pictures were taken periodically as a reference for the true vertical. Then, the measurement software could automatically convert the camera-referenced three-dimensional coordinates to geocentric ones. In exp. C and D, the stereo camera pitch and roll could not be adjusted by motors; however, the orientation of the entire probe was constantly monitored by the pitch and roll sensor, angular measures of which fluctuated by no more than $\pm 0.5^{\circ}$ for each of the axes. The plumb-line images for correcting stereo camera pitch and roll in exp. C and D were taken at 10–20 m depth with a free-hanging probe. These corrections were applicable to pictures taken at greater depths based on the probe pitch and roll sensor data. The probe was suspended on a stiff cable with a single point of attachment and might have rotated back and forth slightly when hanging at rest at the measurement depth. The vessel's dynamic positioning system was used to minimize drift during data collection in exp. C and D. The weather conditions in exp. A were satisfactory (Sea State 4) and very good in exp. C and D (Sea State 1 and 2). The Antarctic krill body tilt orientation data (exp. A) were collected over a period of 5 h (8 pm to 1 am local time; Table 1) with majority of the measurements obtained from encounters of two polarized schools (observed 4 h apart). The *in situ* Northern krill data were collected over three subsequent nights in exp. C and a single night in exp. D (Table 1).

Ex situ exp. B

Photographic images were collected over a 3-d period at the Austevoll Aquaculture Research Station in Norway (Table 1). A specially designed, seawater-filled cylindrical enclosure (or mesocosm) was installed on a floating raft, moored 30 m offshore (Figure 5b). The enclosure was made of 0.45 mm thick black opaque woven-coated polyethylene. Seawater was pumped through tubes from 160 m depth in the nearby fjord, sand-filtered, monitored with respect to oxygen, temperature, and salinity, and delivered through a pre-installed water spreader to the central bottom part of the enclosure at a rate of 14 l/min (~15% of water volume exchange per 24 h). The outlet was installed in the enclosure wall ~20 cm below the water surface. The installation was covered with black plastic sheets to simulate lasting darkness. The stereo camera and flash units were attached to a 40-mm diameter steel pipe which was lowered 4 m into the enclosure, positioned close to its wall, then firmly attached to the raft. The cameras were horizontally oriented towards the centre of the mesocosm. A low-light sensitive video camera (Kongsberg OE15-100C-0005) was mounted beside the flash units to aid the monitoring of krill behaviour.

Northern krill caught in the nearby fjord (Table 1) were stored for 9 d in two opaque 500-l storage tanks installed on the raft next to the enclosure (Figure 5b). A substantial amount of smaller planktonic organisms (mainly copepods) were caught together with the krill and were available to feed upon during the period of krill storage in tanks. The plastic storage tanks were covered by lids and totally

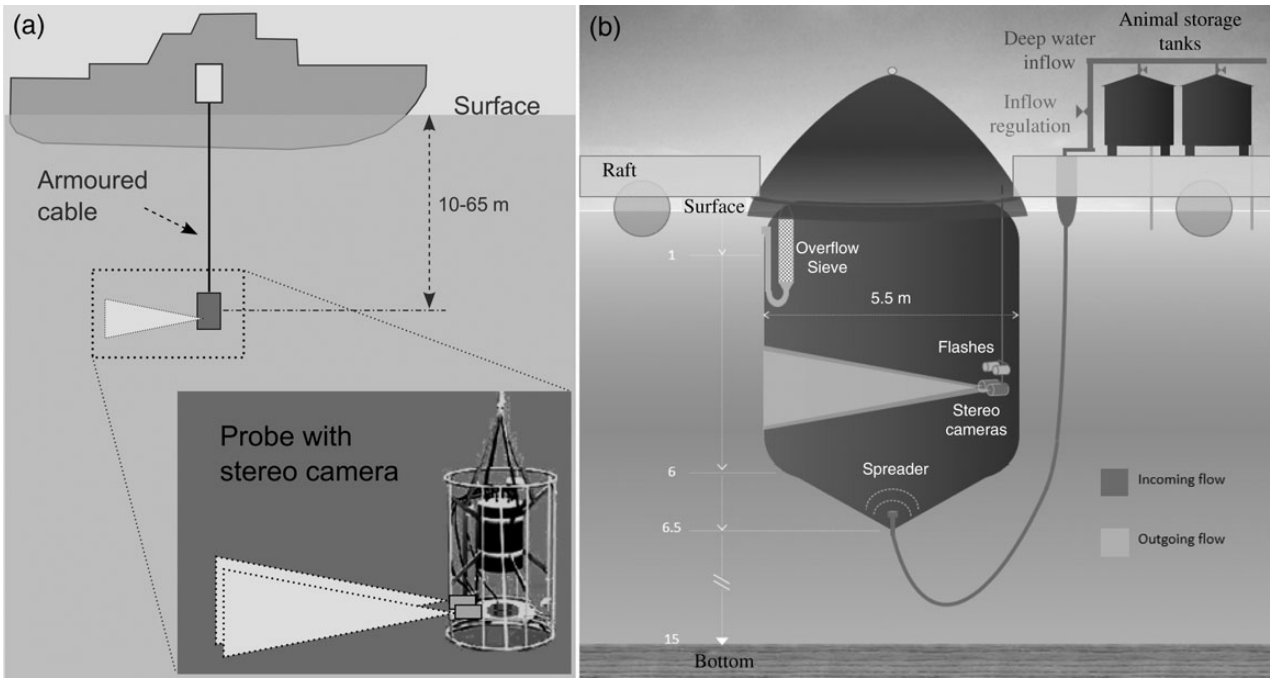

Figure 5. (a) Sketch of the set-up with a stereo camera mounted on an acoustic probe and deployed from the research vessel using an armoured cable (exp. A, C, and D). (b) Sketch of the mesocosm cylindrical enclosure for exp. B.

opaque. A steady flow of seawater (4 l/min) was supplied from the same source that fed the mesocosm. About 100 animals were carefully introduced into the mesocosm several hours before image data collection.

Results

The raw data analysed comprise >4200 stereo photo image pairs with about equal contributions from exp. B and C (combined ~3600 stereo pairs), ~400 from exp. D, and 200 from exp. A. A few polarized schools of Antarctic krill were observed in exp. A (couple of pictures per school; Figure 1) with very few and scattered animals when no school in sight. The Northern krill, on the other hand, were observed and measured at low volume densities, as solitary individuals with no obvious coordinated movement (exp. B, C, and D). More than 1000 individual Northern krill were identified in exp. B, >600 in exp. C, and >400 in exp. D. After stereo image data filtering for quality, a total number of 542 body tilt orientation and 348 length measures were extracted for Antarctic krill and 403 body tilt and 175 length measures for Northern krill (Figure 6).

The two polarized schools of Antarctic krill analysed within the exp. A seemed to have a fairly similar body orientation distributions [mean of -14.3° ($SD = 14.5^\circ$, $N = 341$) and -23.0° ($SD = 17.0^\circ$, $N = 201$)]. These, for our limited data, were compiled with the result of a negative (head-down) mean measured Antarctic krill body tilt of -17.5° ($SD = 16.0^\circ$; Figure 6a). The mean measured tilt angles of Northern krill were positive (head-up) in exp. B (9.2°) and exp. D (16.8°), but negative in exp. C (-10.5°). The distribution spreads for Northern krill were rather large, but comparable between the datasets (*SD* of 30.6°, 37.5°, and 35.6° for exp. B, C, and D, respectively). The obtained Northern krill body orientation measurement distributions are somewhat bimodal, and generally fail if tested against normality for the datasets collected *in situ* (Table 2). From the limited material here, we did not suggest to fit more advanced distributions. Figure 7 indicates how measured Northern krill body orientation changes with the time of day for exp. B, C, and D. All exp. A measurements were obtained on two schools, i.e. two narrow time intervals (08:00 pm and 00:30 am; not displayed in Figure 7). The exp. B and C data were collected over >24 h; however, there was no substantial difference in body tilts or lengths observed at the same time of day. The exp. B and C orientation and length measurements presented in Figures 6d, e, g, and h and 7 show data pooled over the whole data collection period; 2 and 3 d or ~28 and ~29 h of pooled observation time, respectively.

The length distributions of krill shown in Figure 6c, f, i, and l are from trawl catches associated with exp. A, B, C, and D, respectively. The Antarctic krill (*E. superba*) was the only krill species found in the trawl catch for exp. A. The Northern krill (*M. norvegica*) was also by far the most abundant krill species in the trawl samples for exp. B, C, and D (>99% by the number in exp. C and D and >90% in exp. B); a few *T. raschii*, *T. inermis*, *T. longicaudata*, and *Nyctiphanes couchii* were also caught. The Antarctic krill trawl sample (Figure 6c) was taken at a similar water depth, but 30 h before and 4 km away from the stereo image data collection site. The correspondence of this trawl sampling station data to the camera-based krill length measures could be disputed. Nevertheless, if accept as comparable, the Antarctic krill length measurements from the photographs were not significantly different from the trawl sample length distribution (*t*-test, $p > 0.05$; Figure 6b and c). The Northern krill length distributions measured by stereo camera (AT) and from biological sampling (AT recalculated from TT) were not significantly different in exp. B and C, but they did differ in exp. D. Later is likely caused by the lag time between the acquisition of stereo images and trawl sampling. The trawl sampling and image data collection during exp. C coincided very closely on respect to location, depth, and time (Table 1). The good agreement between the catch-based and image-derived krill length distributions here (Figure 6h and i) validate the effectiveness of our length measurements by a stereo camera. The single trawl sample in exp. D was taken at the same location and water depth as the images, but 7 h later and in daytime. The size-dependent gear avoidance in daytime krill sampling (e.g. Simard and Sourisseau, 2009) is one of likely reasons for significant krill size difference between image-derived and sample data in exp. D (Figure 6k and l). The poor correspondence of the length distributions acquired in exp. B (Figure 6e and f) could partly be explained by unaccounted mortality in the storage tank, as the krill had been stored for 9 d between the trawl sample (Figure 6f) and the stereo camera measurements in the enclosure (Figure 6e).

The Antarctic krill school volume density was measured from an example stereo image pair (one image of the pair is shown in Figure 1) as a demonstration of such stereo camera application. The opportunity for stereo camera deployment was taken when slowly cruising RV "G.O. Sars" (details in Table 1) encountered an Antarctic krill school (Figure 8a) in an area with generally low density of schools. The vessel was stopped and the acoustic probe with a stereo camera was deployed to the relevant depth (20 m) to encounter the crossed-over krill school. In few minutes, a krill school approached the probe and a stereo picture was taken with krill seen at ≥2.0 m range from the camera (Figure 1). A stereo-measurement session (separate from krill body tilt orientation) was performed for this particular stereo-image pair with only the eye of each krill being marked (Figure 8b). The density of krill was favourable for a good quality image analysis at ~2.0–3.5 m range from the camera. However, some krill still did overlap and could not be measured. Therefore, the stereo camera-based krill school volume density measure of 653 ind/m^3 is considered as valid, but likely underestimated to some degree.

Discussion

The example datasets of Antarctic (*in situ*) and Northern krill (*in situ* and *ex situ*) observed by stereo camera were presented and analysed primarily for body orientation, but also for length and school volume density. Doing so, we demonstrate the specific application of the stereogrammetric measurement method for *in situ* animal body orientation measurements, an important parameter in fisheries acoustics. Furthermore, some of the practical considerations of stereo camera use for *in situ* krill body orientation measurements are also discussed.

Data examples: Antarctic and Northern krill

The small number of Antarctic krill schools encountered and low numerical density in the layers of Northern krill together with strict data-quality screening limited the number of acceptable measurements, despite the quite large image dataset that was collected. Though few, these results are listed along with the small number of earlier publications on orientation of free-swimming euphausiids in Table 3. The measured tilt angles were referenced to the true vertical by a plumb-line image (exp. B, C, and D) or motorized platform equipped with a pitch and roll sensor (exp. A). The estimated accuracy of the tilt measurement was about $\pm 1^\circ$, which is satisfactory when compared with the wide spread of the observations as reported here (*SD* of 14–17° for polarized school and ~30–37° for layers of

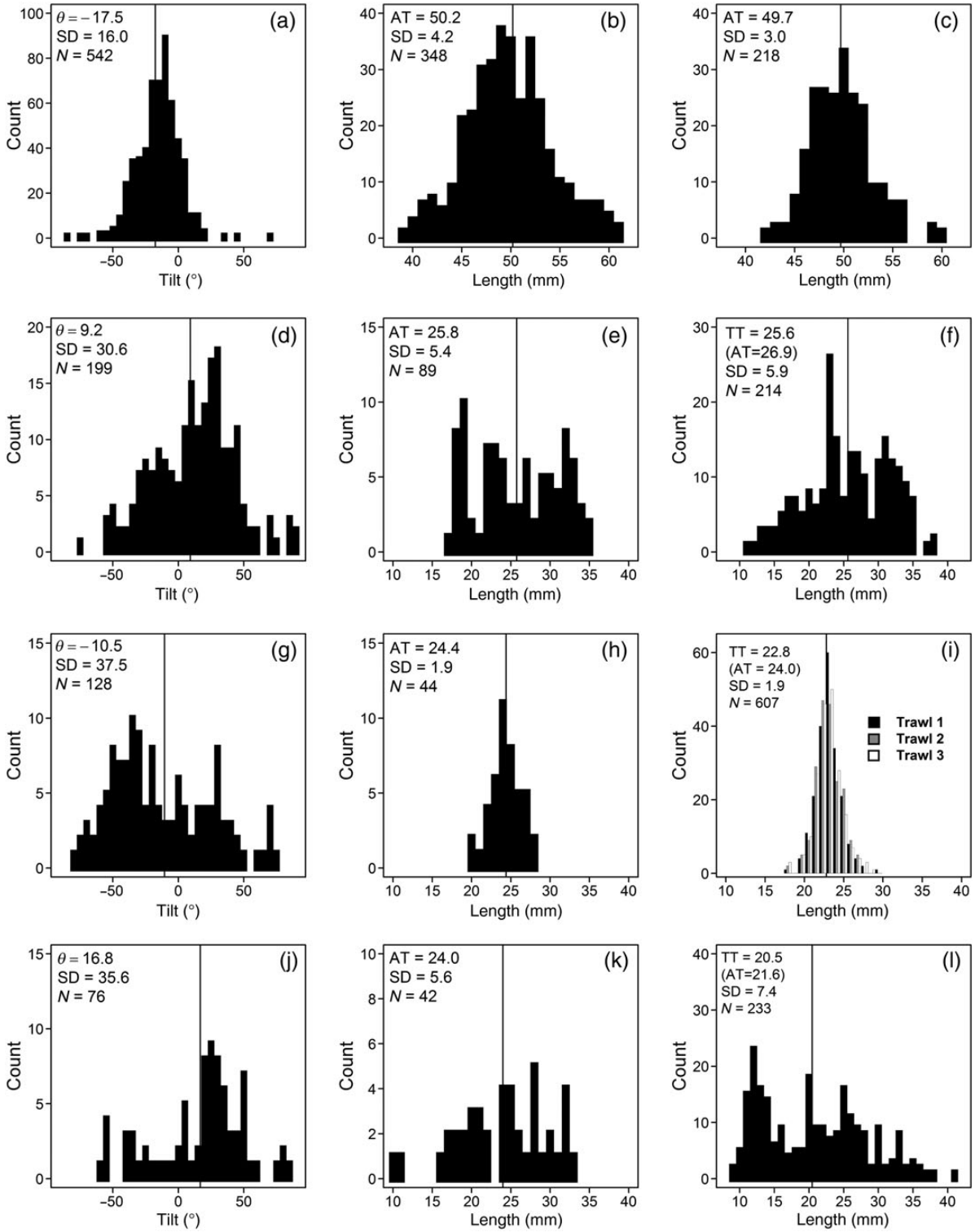

Figure 6. Krill body tilt and length measurements by a stereo camera (first two panel columns) and length distributions obtained from trawl samples. Top row: exp. A (South Atlantic Ocean); Antarctic krill body tilt (a) and length (b) measured by a stereo camera and a corresponding trawl sample (c). Second row: exp. B (*ex situ*); Northern krill body tilt (d) and length (e) as measured over 2 days and nights; (f) representative krill size distribution from four trawl samples for exp. B. Third row: exp. C (Osterfjorden); Northern krill body tilts (g) and lengths (h) as measured over three nights, and the corresponding trawl sample length distributions (i), one trawl haul each night. Bottom row: results from exp. D (Romarheimsfjorden), Northern krill body tilts (j) and lengths (k); (l) the length distribution from a trawl sample at exp. D location. θ—mean body tilt angle in degrees (positive values are head-up); *SD*—standard deviation; AT—mean krill length in mm (anterior edge of the eye to the telson tip); TT—mean krill length in mm (rostrum tip to the telson tip). The lengths AT shown in brackets in (f), (i), and (l) are converted from TT measurements (see text). The vertical black lines in the graphs are mean values.

Table 2. D'Agostino–Pearson normality test results (*p*-values) for Northern krill body orientation measurement distributions.

Test	Exp. B	Exp. C	Exp. D
Omnibus	0.911	0.011	0.095
Skewness	0.667	0.032	0.031
Kurtosity	0.985	0.033	0.813

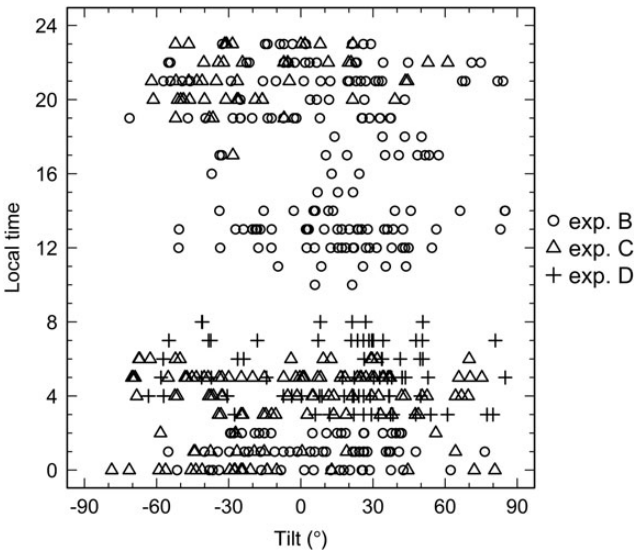

Figure 7. Northern krill body tilt angle vs. time of the day (local time). Data are pooled from measurements over more than 1 d in exp. B and C (see text). Positive tilt is head-up. The time from sunset to sunrise is ~16:00–09:00 hours. Note that exp. B data were collected inside a mesocosm (covered and shaded from direct sunlight).

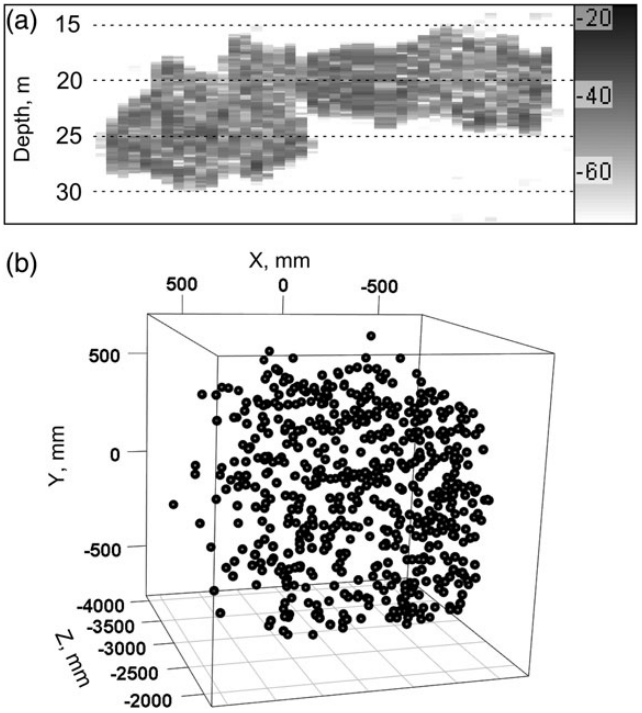

Figure 8. (a) The EK60 200 kHz echogram of Antarctic krill school crossed by RV "G. O. Sars" then targeted by deployed to a 20-m depth probe with cameras (school horizontal length 55 m; colour scale is in dB). (b) Volume density of krill as retrieved from the example pair of stereo images (653 ind/m^3 when zoomed well inside the "cloud"). *Z* is the range in mm from the stereo camera.

scattered animals) or by others (*SD* of ~20–60°; Table 3). The length measurement accuracy in our data was ±0.5–1.6 mm, which is a substantial fraction of the typical Antarctic and Northern krill body length. However, image-derived and trawl-catch length measurements corresponded very well when collected at nearly same location, water depth, and time (exp. C; Figure 6h and i; and Table 1).

There were considerable differences in the observed mean tilt angles between our experiments A, B, C, and D (Figure 6). Krill body is negatively buoyant (Kils, 1981) and animal locomotion is needed to generate a hydrodynamic lift allowing for maintained position in the water column. Except for a special case of krill escape behaviour, a generally positive (head-up) mean tilt of forward moving animal could be expected, as observed in our exp. B and D. However, krill night-time downward migration can at times be well spread over the period of darkness and result in an overall negative mean value, as in exp. C (Figures 6g and 7). Similar euphausiid (mixture of *M. norvegica*, *T. inermis*, and *T. raschii*) behaviour was reported by Kristensen and Dalen (1986), from work in the Norwegian fjords near Tromsø at 02:00 hours local time. The graphically presented results ($N(-9.8; 34.1)$) were temporarily limited (two observations 5 min apart, total sample size 192), but the authors did mention additional krill tilt observations at day and night with comparable measurement where the spread and mean orientation shifted from slightly negative to slightly positive values during the course of the day. Unfortunately, these data were not presented and the proportion of Northern krill in the observed multispecies ensemble was not indicated. Sameoto (1980) also presented *in situ* krill orientation measurements, with Northern krill as the dominant species by numbers, but often mixed with *T. inermis* and *T. raschii*. His krill tilt measurements were obtained during 31 trawl hauls, utilizing a single camera attached to the net. The mean tilt varied greatly (−69° to 86°), based on rather few (1–29) measurements per trawl haul. Generally, Sameoto (1980) reported Northern krill tilts with higher mean values and lower standard deviations than those in our experiments. In a relatively similar manner, Lawson *et al.* (2006) compiled Antarctic krill body orientation measures ($N(9.7; 59.3)$) extracted from data obtained by a video plankton recorder attached to a towed body used over 2 months of vessel transects. Kils (1981) and Endo (1993) reported even higher mean tilt angles for Antarctic and Northern krill, from measurements done in a small aquarium. It is also likely that the confinement in a small water volume could have affected the natural swimming behaviour of the krill. Letessier *et al.* (2013) observed Antarctic krill in a substantially larger aquarium (2.7 m^3) and reported more horizontal mean animal body tilt ($N(23.5; \sim 37)$), which was shifting between slightly negative to higher positive for behavioural modes "feeding", "escape", and "undisturbed", but always with rather large spread of body tilts; similar to one of non-schooling Northern krill reported here (exp. B, C, and D).

In light of the new krill orientations measured in this study, an acoustic *TS* modelling exercise was performed and the predictions compared for krill body orientation measurements reported here

Table 3. Published tilt angle measurements on free-swimming euphausiids, including results from the present study.

Author (year)	Species	Mean tilt[a], *SD* (*N*)	Details
Sameoto (1980)	*M. norvegica* *T. inermis* *T. raschii*	27 – 51, 20 – 27 (230)	*In situ*. Single camera on plankton trawl. 31 trawl hauls. Depth 23 – 164 m. T.: 14:00 – 02:00 hours
Kils (1981)	*E. superba* *M. norvegica*	45.3, 30.4 (1019) 53.8, 64.2 (319)	Aquarium (63 l), single camera
Kristensen and Dalen (1986)	*M. norvegica* *T. inermis* *T. raschii*	−9.8, 34.1 (192)	*In situ*. Single camera at 40 m depth. T.: 02:00 hours
Endo (1993)	*E. superba*	45.6, 19.6 (67) H: 49.7, 7.5 (50)	Aquarium (219 l), single camera
Miyashita *et al.* (1996)	*E. pacifica*	30.4, 19.9 (679) H: 36.9, 12.9 (476)	Aquarium (63 l), single camera
Lawson *et al.* (2006)	*E. superba*	9.7, 59.3 (972)	*In situ*. Video plankton recorder (towed body). Depth 20 – 300 m. T.: 09:00 – 15:00, 17:00 – 07:00 hours
Letessier *et al.* (2013)	*E. superba*	23.5, ∼37 (100)	Aquarium (∼2.7 m^3). Stereo video camera
Exp. A	*E. superba*	−17.5, 16.0 (542)	*In situ*. T: 20:00 – 01:00
Exp. B	*M. norvegica*	9.2, 30.6 (199)	Mesocosm (148 m^3). T.: 10:00 – 02:00 hours
Exp. C		−10.5, 37.5 (128)	*In situ*. T.: 20:00 – 06:00 hours
Exp. D		16.8, 35.6 (76)	*In situ*. T.: 02:00 – 08:00 hours

SD, standard deviation (generally from least-squares fitted normal distributions); *N*, count; H, mean body tilt when hovering; T, local time; "Species", combined results for a mixture of krill species in Sameoto (1980) and Kristensen and Dalen (1986); results for two separately examined krill species in Kils (1981).
[a]Mean tilt from horizontal (0°), positive is head-up. The krill body-axis reference for the measured tilt was not always consistent between authors.

and for several examples from the literature (Figure 9). The stochastic distorted wave Born approximation (SDWBA) model (Demer and Conti, 2003) with successive improvements (Calise and Skaret, 2011) was employed. The standard mean values for input parameters were used as suggested by CCAMLR (2010) and endorsed since 2011 by Commission for the Conservation of Antarctic Marine Living Resources for biomass estimation of Antarctic krill. SDWBA frequency spectrum results are presented for individuals of 25 mm length, as proxy for Northern krill of sizes measured in this study, and 50 mm, which corresponds to the mean length of Antarctic krill measured in exp. A. *TS* predictions at typical echosounder frequencies are also listed (Table 4). The predicted *TS* varies within ∼3 dB (at 70–333 kHz) for different krill body orientation distributions. In general, SDWBA krill *TS* modelling exercise indicated somewhat higher *TS*s for krill orientation measurements reported here compared with the earlier reports in the literature.

The krill-body orientation depends on their behaviour which can vary substantially with diverse activities such as feeding, diel vertical migration, horizontal cruising, and also with external factors like currents, predator avoidance, and reactions to observation platforms (vessels and probes). The diel vertical migration of Northern krill is not limited to simple ascent at dusk and descent ant dawn (Sourisseau *et al.*, 2008; Vestheim *et al.*, 2014), and a significant fraction of the nocturnally feeding population have been observed revisiting the deep water masses (normally occupied at day) and rising, re-joining surface feeding layer during the course of same night. Such behaviour is likely to increase variability and spread of Northern krill natural body orientation distribution. Indeed from our data and other reports (Table 3), it also seems likely that Northern krill has a rather variable swimming behaviour. This is evident from the large spread of tilt measurements around the mean values, but also from the variability of the mean estimates themselves. This behavioural trait is also found among other euphausiid species. The Antarctic krill, on the other hand, is often observed to form large and polarized aggregations with relatively similar individual krill body orientations at a given time instance, which, we speculate, is still likely to be rather dynamic over time. However, there is some indication that Antarctic krill body orientation distribution has a sizable spread even within the borders of a single school (exp. A, $SD = 14–17°$). Though empirical euphausiid tilt angle distributions generally have a quite large *SD*, it is notable that rather narrow distributions have been adopted in theoretical model studies of the acoustic backscattering by krill (e.g. Demer and Conti, 2005; Conti and Demer, 2006; McQuinn *et al.*, 2013), intended to predict mean *TS*s for biomass estimation purposes (Demer and Conti, 2005). The current state-of-the-art model for Antarctic krill biomass estimation use a more variable distribution of orientation [$SD = 28°$, CCAMLR (2010)], which, notably, is not confirmed by direct measurements of krill orientation *in situ*.

The body tilt as a measured angle between the horizontal plane and the line along the dorsal side of the krill carapax is commonly used in *TS* modelling exercises (e.g. McGehee *et al.*, 1998; Demer and Conti, 2005; Amakasu and Furusawa, 2006). However, this is not practical for analysis of photo images collected *in situ*; Figure 2b is an example where the line along the dorsal side of the carapax is not a good approximation of the general orientation of the whole animal body. The relationship between later and the more practical body tilt angle definition used in this work is not established, but is likely to be needed when incorporating image-derived krill body tilt parameter into krill *TS* models. A similar morphometric measure, the line between tail and the eye of the krill, was indeed adopted by Lawson *et al.* (2006) to define the orientation of individuals from still digital images obtained by a video plankton recorder as an input parameter for their krill *TS* model.

The obtained Northern krill orientation measurements were normally distributed in exp. B and not normally in exp. C and D (Table 2). The later was perhaps a consequence of relatively small sample sizes. However, a tendency for two modes might also be inferred in our Northern krill orientation data [see also Kristensen and Dalen (1986)] with fewer animals adopting horizontal orientation (Figure 6d, g, and j). The important message rising from our observations, also supported by other investigations, is that the spread is

large and consistently similar for Northern krill (~30–35° if the standard deviation is used as a measure) and possibly sizable even within a single school of Antarctic krill (*SD*=14–17°). The mean Northern krill body orientation, however, may change from slightly head-up to head-down, depending on the specific behaviour adopted (e.g. feeding, resting, or migrating). Therefore, given the *in situ* and *ex situ* data obtained on loose aggregations of *M. norvegica* in this study, it can be suggested that acoustic *TS* modelling should not assume horizontal average animal posture, but rather be based on positive (head-up) or negative mean body tilt of ~10–15° accompanied with fairly broad distribution (*SD* of 30–35°). It should be noted, however, that in exp. B, C, and D, our measurements were obtained over entire night (or day) and more narrow Northern krill body orientation distributions might be observed at specific shorter periods of diel vertical migration. If the rise and glide strategy (Huse and Ona, 1996) is followed, a bimodal tilt angle distribution is expected in most of the situations for negatively buoyant animals. Active midnight downward swimming has also been suggested for a sizable fraction of the feeding Northern krill population, seemingly as a normal part of their diel vertical migration (Sourisseau *et al.*, 2008). The Antarctic krill body tilt measurements were limited in time and space; however, it is interesting that observed within-school krill body tilt variability (two schools) was 2–3 times larger than one found appropriate in earlier krill *TS* modelling for biomass estimation (Demer and Conti, 2005) and almost two times smaller than one used now (CCAMLR, 2010). Further investigations should be made both in laboratory and in field using stereo video analysis tools for detailed description of krill swimming behaviour as started by Kils (1981). If broadband acoustic measurements can be made in conjunction with such analysis, the effect of different behavioural modes may be better understood. Improved target resolution in space and continuous over the frequency spectrum acoustic backscatter measurement would provide with new possibilities for fine scale analysis of krill behaviour, acoustic scattering, and acoustic target identification.

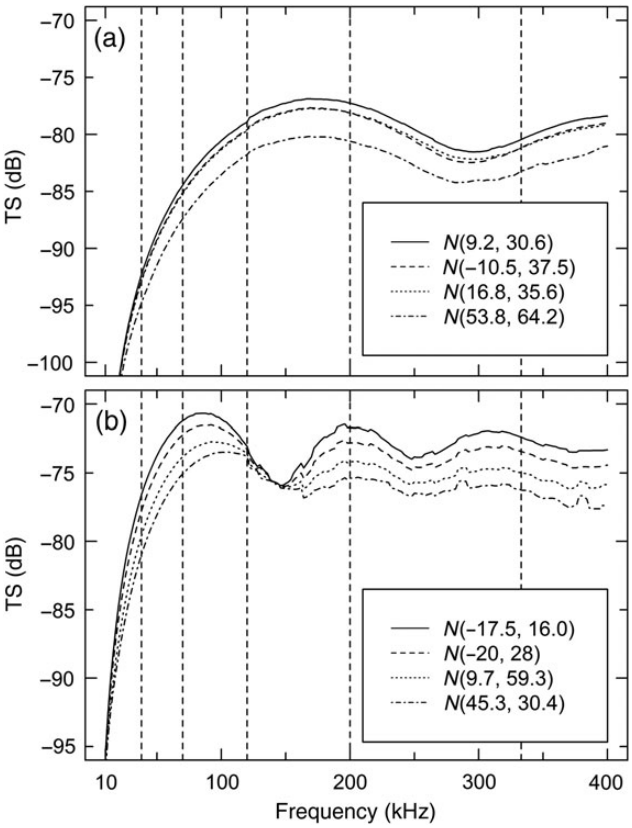

Figure 9. SDWBA *TS* modelling predictions estimated with standard CCAMLR (2010) parameterization for Antarctic krill. (a) Spectrum results for a 25-mm individual (as proxy for Northern krill) with body tilt orientations: *N*(9.2, 30.6) (exp. B), *N*(−10.5, 37.5) [exp. C, similar to *N*(−9.8, 34.1) from Kristensen and Dalen (1986)], *N*(16.8, 35.6) (exp. D), and *N*(53.8, 64.2) (Kils, 1981). (b) Spectrum results for a 50-mm Antarctic krill with body tilt orientations: *N*(−17.5, 16.0) (exp. A), *N*(−20, 28) (CCAMLR, 2010), *N*(9.7, 59.3) (Lawson *et al.*, 2006), and *N*(45.3, 30.4) (Kils, 1981). Vertical lines depict typical echosounder frequencies: 38, 70, 120, 200, and 333 kHz.

Practical considerations

The underwater stereo imaging techniques have been applied in marine science for over 40 years now (Shortis *et al.*, 2009), with probably the most common application of sizing the taxonomically identified animals. The stereo camera-based animal length measurement accuracy is generally superior to single camera systems, especially for animals observed with less favourable body postures (Harvey *et al.*, 2002). However, the stereo-measurement technique is still largely unused for quantifying the natural body tilt orientation distributions of free-swimming euphausiids (Table 3). Based on practical experience from several krill orientation measurement experiments (Table 1), we suggest to use the krill body dimension AT [anterior edge of the eye to tip of the telson; Figure 2b; also used by Letessier *et al.* (2013)] as a basis for *in situ* krill body tilt orientation

Table 4. SDWBA model *TS* predictions (dB) at typical survey echosounder frequencies for krill of 25 mm (as proxy for Northern krill in this study) and 50 mm length (as appropriate for Antarctic krill in this study), using standard input parameters (CCAMLR, 2010) and at body orientation distributions reported here and by others.

			Frequency (kHz)				
Length (mm)	**Orientation *N*(mean, *SD*) (degrees)**	**Source**	**38**	**70**	**120**	**200**	**333**
25	*N*(9.2, 30.6)	Exp. B	−92.3	−84.5	−78.9	−77.3	−80.5
	N(−10.5, 37.5)	Exp. C[a]	−92.8	−85.1	−79.6	−78.1	−81.2
	N(16.8, 35.6)	Exp. D	−92.9	−85.2	−79.7	−78.1	−81.2
	N(53.8, 64.2)	Kils (1981)	−94.8	−87.4	−81.8	−80.6	−83.2
50	*N*(−17.5, 16.0)	Exp. A	−76.6	−71.2	−73.1	−71.7	−72.4
	N(−20, 28)	CCAMLR (2010)	−77.8	−72.2	−73.3	−72.8	−73.4
	N(9.7, 59.3)	Lawson *et al.* (2006)	−79.6	−73.8	−73.6	−74.2	−75.0
	N(45.3, 30.4)	Kils (1981)	−81.0	−75.1	−73.8	−75.4	−76.2

[a]Similar to *N*(−9.8, 34.1) in Kristensen and Dalen (1986).

measurements with a stereo camera. If similar to ours equipment and set-up used, it is advised to limit the krill body tilt measurements to animals with body yaw angle of no more than ± 40–50°, depending on krill body-to-image-background contrast [Figures 2b–4; an issue not discussed by Letessier *et al.* (2013)]. The stereo photo unit consisting of two commercial underwater ROV cameras was used here. Though identical and originating in the same factory production batch, our photo cameras responded to a single sent trigger signal with small, but variable between the two cameras, time delay. This severely limited the number of well-illuminated stereo photograph pairs when using a single flash unit connected to one of the two cameras (exp. A), but a small time difference in-between two images of the single stereo pair was present, if two camera flash units used (0.037 s in exp. B, C, and D). The latter problem was not a restriction for a slow moving animal such as Northern krill. However, this challenge can be solved completely by having a single flash unit with an adjustable flash event delay after camera triggering signal and a longer image exposure time would be appropriate in low ambient light levels such as found at water layers occupied by Northern krill at day (deep) and at night. The stereo video system, however, would probably be advantageous at higher ambient light levels, as suggested by Letessier *et al.* (2013) who advocated daytime observations of Antarctic krill in shallow waters based on their results in a tank. Referencing the target orientation to the true vertical in geocentric space is a highly relevant issue to consider when measuring *in situ* [not discussed by Letessier *et al.* (2013)]. We addressed this challenge in two ways: (i) a stereo camera attached to a probe with a motorized, equipped with a pitch and roll sensor platform that could be remotely adjusted and constantly monitored to ensure the horizontal orientation of the stereo camera; (ii) use the orientation of a suspended in the field of view plumb-line as an input for the PhotoMeasure software to reference the krill body tilt measures to the geocentric space. The first approach requires some amount of additional purpose-build equipment, while second also returned satisfactory results and can be sufficiently practical when pitch–roll sensor is not available.

Acknowledgements

The crews of RV "G.O. Sars", RV "Håkon Mosby", RV "Hans Brattstrøm", and Austevoll Research Station (Norway) personnel are thanked for their cooperation during the work. Ronald Pedersen (IMR) is thanked for his effort when collecting Antarctic krill data. James Seager is thanked for his effort when producing camera calibration files for exp. A. Tor Knutsen (IMR) is thanked for his help during Northern krill sampling. The Research Council of Norway is thanked for its financial contribution to the WESTZOO project (no. 190318/S40) and industrial PhD project (no. 212113/O30). The Marine Ecosystem Technologies AS Company is thanked for its financial contribution to industrial PhD project (no. 212113/O30). All AKES (2008) survey contributors are also thanked (Royal Norwegian Ministry of Fisheries and Coastal Affairs, Institute of Marine Research, University of Bergen, Norwegian Antarctic Research Expeditions, Research Council of Norway, Norsk Hydro, Norwegian Petroleum Directorate, and ABB Norway).

References

Amakasu, K., and Furusawa, M. 2006. The target strength of Antarctic krill (*Euphausia superba*) measured by the split-beam method in a small tank at 70 kHz. ICES Journal of Marine Science, 63: 36–45.

Atkinson, A., Siegel, V., Pakhomov, E. A., Jessopp, M. J., and Loeb, V. 2009. A re-appraisal of the total biomass and annual production of Antarctic krill. Deep Sea Research Part I: Oceanographic Research Papers, 56: 727–740.

Calise, L. 2009. Multifrequency acoustic target strength of Northern krill. Department of Physics and Technology, University of Bergen, Bergen, p. 338. https://bora.uib.no/handle/1956/3885.

Calise, L., and Knutsen, T. 2012. Multifrequency target strength of northern krill (*Meganyctiphanes norvegica*) swimming horizontally. ICES Journal of Marine Science, 69: 119–130.

Calise, L., and Skaret, G. 2011. Sensitivity investigation of the SDWBA Antarctic krill target strength model to fatness, material contrast and orientation. CCAMLR Science, 18: 97–122.

Cappo, M. C., Harvey, E. S., and Shortis, M. 2007. Counting and measuring fish with baited video techniques—An overview. *In* Proceedings of the Australian Society for Fish Biology workshop, pp. 101–114. Ed. by D. Furlani, and J. P. Beumer. Australian Society of Fish Biology, Hobart.

CCAMLR. 2010. Report of the fifth meeting of the subgroup on acoustic survey and analysis methods. ICES Document SC-CAMLR-XXIX/6. 25 pp.

Cochrane, N. A., Sameoto, D., Herman, A. W., and Neilson, J. 1991. Multiple-frequency acoustic backscattering and zooplankton aggregations in the inner Scotian Shelf basins. Canadian Journal of Fisheries and Aquatic Sciences, 48: 340–355.

Conti, S. G., and Demer, D. A. 2006. Improved parameterization of the SDWBA for estimating krill target strength. ICES Journal of Marine Science, 63: 928–935.

Cresswell, K. A., Tarling, G. A., Thorpe, S. E., Burrows, M. T., Wiedenmann, J., and Mangel, M. 2009. Diel vertical migration of Antarctic krill (*Euphausia superba*) is flexible during advection across the Scotia Sea. Journal of Plankton Research, 31: 1265–1281.

Cullen, J. M., Shaw, E., and Baldwin, H. A. 1965. Methods for measuring the three-dimensional structure of fish schools. Animal Behaviour, 13: 534–543.

Demer, D. A., and Conti, S. G. 2003. Reconciling theoretical versus empirical target strengths of krill: effects of phase variability on the distorted-wave Born approximation. ICES Journal of Marine Science, 60: 429–434.

Demer, D. A., and Conti, S. G. 2005. New target-strength model indicates more krill in the Southern Ocean. ICES Journal of Marine Science, 62: 25–32.

Dolphin, W. F. 1987. Prey densities and foraging of humpback whales, *Megaptera novaeangliae*. Experientia, 43: 468–470.

Einarsson, H. 1945. Euphausiacea I. Northern Atlantic Species. Dana Report, 27: 1–184.

Endo, Y. 1993. Orientation of Antarctic Krill in an aquarium. Nippon Suisan Gakkaishi, 59: 465–468.

Foote, K. G. 1980. Effect of fish behaviour on echo energy: The need for measurements of orientation distributions. ICES Journal of Marine Science, 39: 193–201.

Foote, K. G., and Stanton, T. K. 2000. Acoustical methods. *In* ICES Zooplankton Methodology Manual, pp. 223–258. Ed. by R. Harris, P. Wiebe, J. Lenz, H. R. Skjoldal, and M. Huntley. Academic Press, London.

Greenlaw, C. F. 1977. Backscattering spectra of preserved zooplankton. Journal of Acoustical Society of America, 62: 44–52.

Greenlaw, C. F., Johnson, R. K., and Pommeranz, T. 1980. Volume scattering strength predictions for Antarctic Krill (*Euphausia superba* Dana). MEERESFORSCH, 28: 48–55.

Harvey, E., Shortis, M., Stadler, M., and Cappo, M. 2002. A comparison of the accuracy and precision of measurements from single and stereo-video systems. Marine Technology Society Journal, 36: 38–49.

Haslett, R. W. G. 1977. Automatic plotting of polar diagrams of target strength of fish in roll, pitch and yaw. Rapports et Procès-Verbaux des Réunions du Conseil International pour l'Exploration de la Mer, 170: 74–81.

Holliday, D. V., Pieper, R. E., and Kleppel, G. S. 1989. Determination of zooplankton size and distribution with multifrequency acoustic technology. ICES Journal of Marine Science, 46: 52–61.

Holt, E. W. L., and Tattersall, W. M. 1905. Schizopodous Crustacea from the North-East Atlantic Slope. Appendix to the Report on the sea and inland fisheries of Ireland for 1903–1903. Part II. Scientific Investigations, Appendix iv: 99–152.

Hopkins, T. L., Ainley, D. G., Torres, J. J., and Lancraft, T. M. 1993. Trophic structure in open waters of the marginal ice zone in the Scotia-Weddell confluence region during spring (1983). Polar Biology, 13: 389–397.

Huse, I., and Ona, E. 1996. Tilt angle distribution and swimming speed of overwintering Norwegian spring spawning herring. ICES Journal of Marine Science, 53: 863–873.

Kaartvedt, S. 2010. Diel vertical migration behaviour of the Northern Krill (*Meganyctiphanes norvegica* Sars). *In* The Biology of Northern Krill, pp. 255–275. Ed. by G. Tarling. Elsevier Ltd, London. 336 pp.

Kawaguchi, S., King, R., Meijers, R., Osborn, J. E., Swadling, K. M., Ritz, D. A., and Nicol, S. 2010. An experimental aquarium for observing the schooling behaviour of Antarctic krill (*Euphausia superba*). Deep Sea Research Part II: Topical Studies in Oceanography, 57: 683–692.

Kils, U. 1981. The swimming behaviour, swimming performance and energy balance of Antartic krill, *Euphasia superba*. BIOMASS Scientific Series, 3: 122.

Klevjer, T., and Kaartvedt, S. 2006. In situ target strength and behaviour of northern krill (*Meganyctiphanes norvegica*). ICES Journal of Marine Science, 63: 1726–1735.

Klimley, A. P., and Brown, S. T. 1983. Stereophotography for the field biologist: Measurement of lengths and three-dimensional positions of free-swimming sharks. Marine Biology, 74: 175–185.

Kristensen, Å., and Dalen, J. 1986. Acoustic estimation of size distribution and abundance of zooplankton. Journal of Acoustical Society of America, 80: 601–611.

Lancraft, T. M., Reisenbichler, K. R., Robison, B. H., Hopkins, T. L., and Torres, J. J. 2004. A krill-dominated micronekton and macrozooplankton community in Croker Passage, Antarctica with an estimate of fish predation. Deep Sea Research Part II: Topical Studies in Oceanography, 51: 2247–2260.

Lawson, G. L., Wiebe, P. H., Ashjian, C. J., Chu, D., and Stanton, T. K. 2006. Improved parameterization of Antarctic krill target strength models. Journal of Acoustical Society of America, 119: 232–242.

Letessier, T. B., Kawaguchi, S., King, R., Meeuwig, J. J., Harcourt, R., and Cox, M. J. 2013. A robust and economical underwater stereo video system to observe antarctic krill (*Euphausia superba*). Open Journal of Marine Science, 3: 148–153.

Mauchline, J. 1980. The biology of mysids and euphausiids. Advances in Marine Biology, 18: 1–681.

Mauchline, J., and Fischer, L. R. 1967. Distribution of the euphausiid crustacean *Meganyctiphanes norvegica* (M. sars). Limnology and Oceanography, 13: 727–728.

Mauchline, J., and Fischer, L. R. 1969. The biology of euphausiids. Advances in Marine Biology, 7: 1–454.

McGehee, D. E., O'Driscoll, R. L., and Traykovski, L. 1998. Effects of orientation on acoustic scattering from antarctic krill at 120 kHz. Deep Sea Research Part II: Topical Studies in Oceanography, 45: 1273–1294.

McQuinn, I. H., Dion, M., and St. Pierre, J-F. 2013. The acoustic multifrequency classification of two sympatric euphausiid species (*Meganyctiphanes norvegica* and *Thysanoessa raschii*), with empirical and SDWBA model validation. ICES Journal of Marine Science, 70: 636–649.

Miyashita, K., Aoki, I., and Inagaki, T. 1996. Swimming behaviour and target strength of isada krill (*Euphausia pacifica*). ICES Journal of Marine Science, 53: 303–308.

Miyashita, K., Aoki, I., Seno, K., Taki, K., and Ogishima, T. 1997. Acoustic identification of isada krill, *Euphausia pacifica* Hansen, off the Sanriku coast, north-eastern Japan. Fisheries Oceanography, 6: 266–271.

Morris, D. J., Watkins, J. L., Ricketts, C., Buchholz, F., and Priddle, J. 1988. An assessmant of the merits of length and weight measurements of Antarctic krill Euphausia superba. British Antarctic Survey Bulletin, 79: 27–50.

Nakken, O., and Olsen, K. 1977. Target strength measurements of fish. Rapports et Procès-Verbaux des Réunions du Conseil International pour l'Exploration de la Mer, 170: 52–69.

Onsrud, M. S. R., and Kaartvedt, S. 1998. Diel vertical migration of the krill *Meganyctiphanes norvegica* in relation to physical environment, food and predators. Marine Ecology Progress Series, 171: 209–219.

Sameoto, D. D. 1980. Quantitative measurements of euphausiids using a 120-kHz sounder and their in situ orientation. Canadian Journal of Fisheries and Aquatic Sciences, 37: 693–702.

SeaGis. 2014. CAL and PhotoMeasure—stereo camera calibration and stereophotogrammetric measurement software packages. http://www.seagis.com.au/index.html (date last accessed 15 December 2014).

Shortis, M., Harvey, E., and Abdo, D. 2009. A review of underwater stereo-image measurement for marine biology and ecology applications. *In* Oceanography and Marine Biology: An Annual Review, pp. 257–292. Ed. by R. N. Gibson, R. J. A. Atkinson, and J. D. M. Gordon. CRC Press, Boca Raton. 360 pp.

Simard, Y., and Harvey, M. 2010. Predation on Northern krill (*Meganyctiphanes norvegica* Sars). *In* The biology of Northern Krill, pp. 277–306. Ed. by G. Tarling. Elsevier Ltd, London. 336 pp.

Simard, Y., and Sourisseau, M. 2009. Diel changes in acoustic and catch estimates of krill biomass. ICES Journal of Marine Science, 66: 1318–1325.

Simmonds, E. J., and MacLennan, D. N. 2005. Fisheries Acoustics: Theory and Practice. Blackwell Science, Oxford. 437 pp.

Sourisseau, M., Simard, Y., and Saucier, F. J. 2008. Krill diel vertical migration fine dynamics, nocturnal overturns, and their roles for aggregation in stratified flows. Canadian Journal of Fisheries and Aquatic Sciences, 65: 574–587.

Stanton, T. K., Chu, D., Wiebe, P. H., and Clay, C. S. 1993. Average echoes from randomly oriented random-length finite cylinders: Zooplankton models. Journal of the Acoustical Society of America, 94: 3463–3472.

Tarling, G. A., Ensor, N. S., Fregin, T., Goodall-Copestake, W. P., and Fretwell, P. 2010. An introduction to the biology of Northern krill (*Meganyctiphanes norvegica* Sars). *In* The Biology of Northern Krill, pp. 1–40. Ed. by G. Tarling. Elsevier Ltd, London. 336 pp.

Vestheim, H., Rostad, A., Klevjer, T. A., Solberg, I., and Kaartvedt, S. 2014. Vertical distribution and diel vertical migration of krill beneath snow-covered ice and in ice-free waters. Journal of Plankton Research, 36: 503–512.

Watkins, J. L., and Brierley, A. S. 2002. Verification of the acoustic techniques used to identify Antarctic krill. ICES Journal of Marine Science, 59: 1326–1336.

Woodd-Walker, R. S., Watkins, J. L., and Brierley, A. S. 2003. Identification of Southern Ocean acoustic targets using aggregation backscatter and shape characteristics. ICES Journal of Marine Science, 60: 641–649.

Zhou, M., and Dorland, R. D. 2004. Aggregation and vertical migration behavior of *Euphausia superba*. Deep Sea Research Part II: Topical Studies in Oceanography, 51: 2119–2137.

Handling editor: Stéphane Plourde